Down-regulation of Phospholipase D Stimulates Death of Lung Cancer Cells Involving Up-regulation of the Long ncRNA *ANRIL*

YEON-HO KANG*, DONGKYUN KIM* and EUN-JUNG JIN

Department of Biological Sciences, College of Natural Sciences, Wonkwang University, Iksan, Republic of Korea

Abstract. *Dysregulation of phospholipase D (PLD) has been found in several types of human cancer, but the underlying regulatory mechanism remains poorly-understood. Herein we found PLD inhibition in human H460 lung cancer cells has anti-tumorigenic effects such as stimulation of apoptosis and autophagy. In the present study, in order to identify the responsible key regulator of these anti-tumorigenic effects of PLD inhibition, we analyzed the expression levels of 90 long non-coding RNAs (lncRNAs). Among them, the expression level of antisense noncoding RNA in the INK4 locus (ANRIL) was increased up to 13.6-fold by PLD inhibition in H460 human lung cancer cells. Moreover, knockdown of ANRIL using its specific small-interfering RNA significantly suppressed PLD inhibition-induced apoptosis. Collectively, our findings showed that ANRIL is an lncRNA responsible in anti-tumorigenesis caused by PLD inhibition and combined incorporation of ANRIL into PLD inhibition-induced anti-tumorigenic signaling network could be a new effective therapeutic approach for controlling lung cancer.*

Phospholipase D (PLD) produces phosphatidic acid (PA), the regulator of mammalian target of rapamycin (mTOR) stability, by the hydrolysis of phosphatidylcholine (1) and exists in two PLD isoforms, PLD1 and PLD2 that display different regulatory and functional mechanism in most mammalian tissues (2). Aberrant PLD/PA signaling has been observed in a number of human carcinoma types, including breast, ovarian, kidney and colonic cancer (3, 4). Elevated PLD activity in human carcinomas is thought to promote cell proliferation and to suppress the default apoptotic programs, thereby promoting cancer growth. However, the underlying regulatory mechanism in PLD-mediated carcinogenesis is still unclear.

Many advanced studies suggest that non-coding RNA (ncRNA) plays an important role in physiological and pathological conditions such as cancer (5). A number of miRNAs such as miR-10b (1), -21 (6), -27a (7), -122 (8), and -132 (9) are known as oncomiRs and have been shown to be involved in metastasis and cell proliferation, as well as cell survival in lung cancer. In recent years, long non-coding RNAs (lncRNAs) have been drawing the most attention in several cancer types and emerging evidence suggests that lncRNAs are broadly implicated in the regulation of genes which in turn regulate major pathways of cell growth, proliferation, differentiation and survival (10). Alteration of specific lncRNAs promotes tumor formation, progression, and metastasis of cancer including prostate and bladder cancer (11-13). Overexpression of prostate cancer antigen-3 lncRNA in malignant prostate tissue (14), metastasis-associated lung adenocarcinoma transcript 1 (MALAT1) and maternally expressed 3 (MEG3) in bladder cancer (15, 16), and homeobox (HOX) transcript antisense intergenic RNA (HOTAIR) in small cell lung cancer (17) have been discovered. Besides regulation of gene expression, certain lncRNAs are known to act as miRNA 'sponges' (18) and some, such as H19, are host genes for small non-coding RNAs that are known to be dysregulated in cancer (19). These reports suggest the clinical relevance of lncRNA in cancer and implicate the possibility of lncRNA as a therapeutic target for controlling cancer. However, the functions of most lncRNAs are still unknown. Therefore, further experimental evidence of the involvement of lncRNA in cancer could allow for a better understanding over tumorigenesis and probable use in clinical practice.

Herein, we aimed to evaluate the effect of PLD inhibition and to identify a responsible molecule for providing a possible new therapeutic approach for lung cancer treatment.

*These Authors contributed equally to this study.

Correspondence to: Eun-Jung Jin, Ph.D., Department of Biological Sciences, College of Natural Sciences, Wonkwang University, Iksan, Chunbuk, 570-749, Korea. Fax: +82 638578837, e-mail: jineunjung@wku.ac.kr

Key Words: PLD inhibitor, LncRNA, ANRIL, H460 cells, lung cancer.

Materials and Methods

Cell line and cell culture. H460 to HCC, H1975 and human colorectal adenocarcinoma cell line HCT116 were grown in RPMI-1640 medium (ATCC) supplemented with 10% fetal bovine serum (Gibco Invitrogen, Carlsbad, CA, USA) and 10 U/ml penicillin–streptomycin (Gibco Invitrogen). The human bronchial epithelial cell line BEAS2B was grown in BEBM medium (Lonza, Basel, Switzerland) supplemented with 10% fetal bovine serum (Gibco Invitrogen, Carlsbad, CA, USA) and 10 U/ml penicillin–streptomycin (Gibco Invitrogen). All of these cells were purchased from the American Type Culture Collection (ATCC: Rockville, MD, USA). Cells were cultured in RPMI-1640 medium (ATCC) supplemented with 10% fetal bovine serum (Gibco Invitrogen, Carlsbad, CA, USA) and 10 U/ml penicillin–streptomycin (Gibco Invitrogen). Cells were maintained in a humidified incubator at 37˚C with 5% CO_2. For this study, cells were treated with 3 μM gefitinib (Selleck Chemicals, Houston, TX, USA), 30 μM parthenolide (Sigma-Aldrich, St. Louis, MO, USA) and 30 μM PLD 1/2 inhibitor FIPI (EMD Millipore, Billerica, MA, USA).

Crystal violet staining. Cells were seeded at 10^4 cells/well in 24-well plates and incubated for 12 h. Cells were then treated with PLD 1/2 inhibitor at different concentrations (0, 10, 20, 30 and 50 μM) for 48 h. After treatment, cell culture medium was removed and cells fixed with methanol. Cells were stained by 0.5% (w/v) crystal violet and destained with 1% Triton X-100 (AMRESCO, Cochran Road Solon, OH, USA) in phosphate-buffered saline. The absorbance was then read at a wavelength of 500 nm on a SUNRISE spectrophotometer (TECAN, Männedorf, Switzerland).

Mitochondrial membrane potential assay. The mitochondrial depolarization state of treated cells was assessed using a Muse cell analyzer (Merck Millipore, Darmstadt, Germany) using mitopotential assay kit (EMD Merk Millipore, Billerica, MA, USA). Briefly, both floating and adherent treated cells were collected, centrifuged at 300× *g* for 5 min, and then a 100 μl aliquot of cell suspension was first added to 95 μl of diluted Muse MitoPotential dye, and after 20 min at room temperature, addition of 5 μl 7-Aminoactinomycin D reagent dye was carried out. After 5 min, the percentage of live, depolarized, and dead cells in the cell suspensions was measured immediately using a Muse® cell analyzer (EMD Merk Millipore).

Cell apoptosis assay. Cultured lung cancer H460 cells were treated with Dimethyl sulfoxide or PLD 1/2 inhibitor for 48 h. Cells were then incubated with 100 μl of Annexin V and dead cell detection reagent (EMD Merk Millipore, Billerica, MA, USA) at room temperature for 20 min and apoptosis was measured using a Muse cell analyzer (EMD Merk Millipore)

Western blot. Treated and control cells were lysed in RIPA buffer (Cell Signaling, Beverly, MA, USA) for 30 min on ice. The total protein content of the cells was determined by the BCA protein assay kit (Pierce Biotechnology Inc., Rockford, MN, USA). Proteins (30 μg) were separated by 10% polyacrylamide gel electrophoresis containing 0.1% sodium dodecyl sulfate and transferred to nitrocellulose membranes (GE Health Care, Buckinghamshire, UK). The membranes were incubated for 1 h at room temperature in a blocking buffer (20 mM Tris-HCl, 137 mM NaCl, pH 8.0, containing 0.1% Tween and 2% Bovine serum albumin), and antibodies against coiled-coil myosin-like BCL2-interacting protein (BECLIN-1; Cell Signaling), microtubule-associated protein 1 light chain 3 alpha (LC3A; Cell Signaling), microtubule-associated protein 1 light chain 3 beta (LC3B; Cell Signaling), autophagy-related gene 3 (ATG3; Cell Signaling), autophagy-related gene 5 (ATG5; Cell Signaling) and Glyceraldehyde-3-phosphate dehydrogenase (GAPDH; Santa Cruz Biotech., Santa Cruz, CA, USA).The blots were developed with a peroxidase-conjugated secondary antibody and reacted proteins were visualized using an electrochemiluminescence (ECL) system (GE Health Care).

Fluorescence in situ hybridization (FISH). Tissue array slides containing selected areas of paraffin-embedded sections from primary lung carcinomas, benign lung tissues and lymph node metastases was obtained from SuperBioChips Laboratories (Daejeon, Korea). Dehydrated tissue array slides were incubated in 20% sodium bisulfate/2× Saline Sodium Citrate buffer at 45˚C for 20 min, then treated with 20 μg/ml proteinase K at 37˚C for 10 min and post-fixed with 4% paraformaldehyde for 10 min. After denaturation, hybridization, and post-hybridization washing, sections were counterstained with 4',6-diamidine-2'-phenylindole dihydrochoride in antifade solution (Vector Laboratories, Burlingame, CA, USA) and examined under a confocal microscope (Olympus, Tokyo, Japan). *Antisense non-coding RNA in the INK4 locus* (*Anril*) DNA probe was designed by ncRNA Expression Database (NRED; http://nred.matticklab.com/cgi-bin/ncrnadb.pl) and produced by Bioneer (Daejeon, Korea). The oligonucleotides used as sequence were as follows: *Anril*; 5'-ACTTGAAGATGGTGAAGGAATATAAAAATCTATGTCTCACAGTCCAGACTTGGAGTACAA-3'

LncRNA profiling and data analysis. LncRNA Profiler (System Biosciences, Mountain view, CA, USA) was used for analyzing lncRNA expression. Total RNA was isolated using RNAiso Plus (TaKaRa, Otsu, Shiga, Japan). Tail and tag cDNA were synthesized with Human LncRNA Profiler qPCR Array Kit (System Biosciences, Mountain view, CA, USA) and real-time polymerase chain reaction (PCR) was performed consisting of an initial denaturation step at 95˚C for 10 min, followed by 40 cycles of 15 s at 95˚C, and 1 min at 60˚C using Maxima SYBR Green/ROX qPCR Master Mix 2X (Thermo Scientific, Pittsburgh, PA, USA). Data were analyzed and visualized using a GenEx software (Weihenstephan, Germany).

Real-time reverse transcription (RT-PCR). Total RNA was isolated using RNAiso Plus (TaKaRa, Otsu, Shiga, Japan) according to the protocol as described by the manufacturer. Aliquots of total RNA (1 μg) from each sample were reverse-transcribed into cDNA according to the instructions of the PrimeScript 1st strand cDNA Synthesis Kit (TaKaRa). Quantitative real-time PCR was performed using StepOne plus system (Applied Biosystems, Foster City, CA, USA). PCR reactions were prepared and heated to 95˚C for 1 min followed by 40 cycles of denaturation at 95˚C for 10 s, annealing at specific melting temperature for 1 min, and extension at 72˚C for 1 min. Quantification of the PCR signals was achieved by comparing the cycle threshold value (Ct) of the gene of interest with the Ct value of the reference gene GAPDH. The oligonucleotides used as primers were as follows: *ANRIL*: 5'-AGGGCCAGAGTCAAGATTTATG-3' antisense, 5'-CCATGCTCTCAGCCTCATTTA-3' sense, *GAS5*: 5'-GTTACCAGGAGCAGAACCATTA-3' antisence, 5'-

CATTGGCACACAGGCATTAG-3' sense, and *GAPDH*: 5'-GATCATCAGCAATGCCTCCT-3' antisense, 5'-TGTGGTCATGAG TCCTTCC A-3' sense.

siANRIL transfection. siRNAs were obtained from Bioneer. The target mRNA sequences for the siRNAs were as follows: 5'-GAACCAGGACUGGAACCUA-3'. H460 cells were transfected with 100 nmol of the siRNA using Lipofectamine 2000 (Lipofectamine™ 2000; Invitrogen). Optimization of siRNA/lipofectamine 2000 ratio was carried out as recommended by the manufacturer. The transfected cells were incubated at 37˚C in a humidified CO_2 incubator for 48 h and treated with 0.25% trypsin (Gibco Invitrogen) to harvest for measured apoptosis and mitopotential using Muse analyzer (EMD Merk Millipore, Billerica, MA, USA).

Results

PLD inhibitor stimulates apoptosis and autophagy in H460 cells. To determine whether the PLD inhibitor has antitumor properties, H460 human lung cancer cells were treated with different doses of PLD inhibitor and maintained for three days before cell viability assay using crystal violet. As shown in Figure 1A, blockade of PLD inhibited the growth of H460 cells in a dose-dependent manner. The viability of H460 cells was reduced almost 60% after incubation with 50 μM PLD inhibitor. Moreover, annexin V-positive staining and depolarization of the mitochondrial membrane were also increased with exposure to PLD inhibitor in a dose-dependent manner (Figure 1B). In the presence of 50 μM PLD inhibitor, 60% of cells were recognized as being apoptotic and 80% as being depolarized/dead.

Since PLD catalyzes the hydrolysis of phosphatidylcholine to PA, a key upstream regulator in the mTOR pathway (19), there could be an implication that autophagy might be involved in PLD-mediated carcinogenesis. Inhibition of PLD increased the level of LC3A and LC3B, essential components of autophagic vacuoles (Figure 1C). These data suggest that inhibition of PLD suppresses the growth of H460 cells and induces apoptosis and autophagy, implying its therapeutic potential against human lung cancer.

Inhibition of PLD does not affect the level of growth arrest-specific transcript (GAS5) which is down-regulated in human cancer tissue, rather it modulates the level of ANRIL. Recent research has shown that lncRNA *GAS5* was significantly down-regulated in non-small cell lung cancer and GAS5 acted as a tumor suppressor through key downstream mediators, p53 and E2F transcription factor 1 (E2F1) (20). Herein, we also observed significant down-regulation of *GAS5* in the multitumor tissue arrays composed of 60 lung cancer samples from patients that under no circumstances had undergone chemotherapy before their surgical treatment (Figure 2). Various types of lung cancer, including large cell carcinoma, small cell carcinoma, squamous carcinoma and adenocarcinoma, displayed dramatically lowered *GAS5* expression. However, inhibition of PLD in H460 cells with the indicated dose did not affect the level of GAS5, indicating that anti-tumorigenesis effect *via* PLD inhibition is independent of *GAS5*.

To identify the lncRNA responsible for the anti-tumorigenic effect of PLD inhibition, expression levels of a total of 90 lncRNA transcripts were determined by microarrays. We found that seven lncRNA transcripts were differentially expressed on PLD inhibition, with six being up-regulated and one down-regulated (Figure 3A). Among the dysregulated lncRNA transcripts, *ANRIL* was the one most up-regulated, with a fold change of 13.6. Moreover, the *ANRIL* level was increased with exposure to PLD inhibitor in a dose-dependent manner (Figure 3B). This up-regulation induced by PLD inhibitor was also observed in other human lung cancer cells, such as HCC and H1975 cells (Figure 3C). PLD inhibitor induced *ANRIL* in the human lung-derived BEAS-2B cells (Figure 3D). In addition, *ANRIL* was also up-regulated by PLD inhibitor in HCT116 colorectal cancer cells (Figure 3E). These data suggested that Anril might be the responsible for the anti-tumorigenesis effect by PLD inhibition.

ANRIL is responsible for anti-tumorigenic effect of PLD inhibition. To better understand the significance of *ANRIL* in antitumor actions of PLD inhibitor, we studied whether enforced suppression of *ANRIL* using its specific small interfering RNA (siANRIL) would reverse apoptotic cell death induced by PLD inhibitor. H460 human lung cancer cells were transfected with either with control siRNA or siANRIL to block the expression of *ANRIL*, followed by treatment of 30 mM PLD inhibitor. As shown in Figure 4A, knockdown of *ANRIL* reduced apoptotic cell death (Figure 4A) and de-polarization of the mitochondrial membrane (Figure 4B). With knockdown of *ANRIL*, cell death was reduced to 15% from 45% and the proportion of depolarized dead cells was reduced to 12% from 32%. The expression levels of BECLIN-1, autophagy-related gene 3 (ATG3), autophagy-related gene 5 (ATG5) and LC3B were dramatically increased (Figure 4C). These data suggest an interaction between *ANRIL* and antitumorigenesis by PLD inhibition.

Discussion

Several studies have shown the possible roles of PLD in cancer cells in the context of proliferation, survival, and invasion (21). Overexpression of PLD has been reported to inhibit apoptosis of cancer cells. Herein, we also found that inhibition of PLD stimulates apoptosis and autophagy of H460 human lung cancer cells. However, the molecular mechanism underlying this stimulation of apoptosis and autophagy by PLD inhibition has not been clearly identified. This report

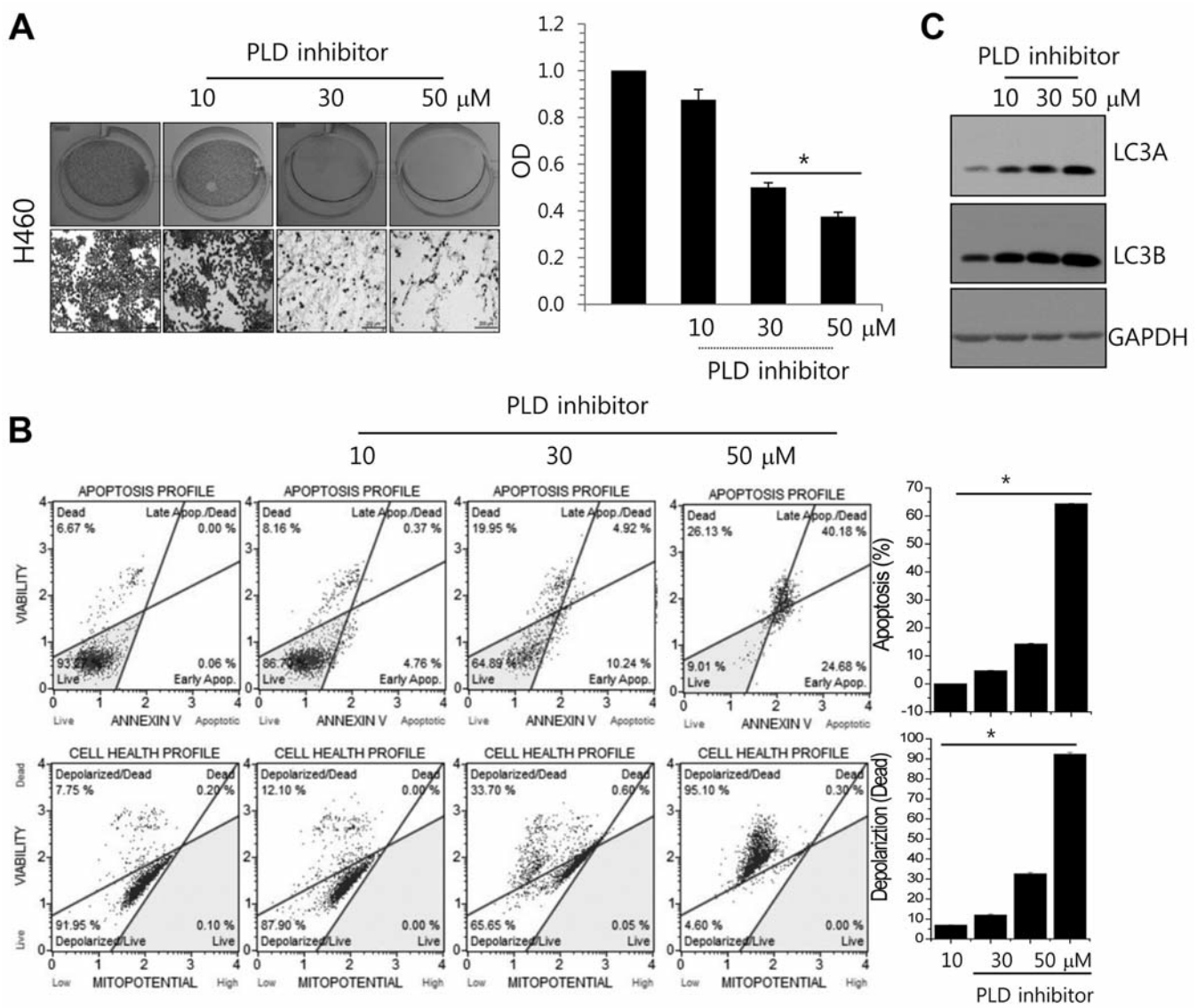

Figure 1. *Phospholipase D (PLD) inhibitor stimulates apotosis and autophagy of H460 human lung cancer cells. A: H460 cells were treated with PLD inhibitor at the indicated concentrations for up to two days amd subjected to crystal violet staining to evaluate cell viability by spectrophotometry at 550 nm. B: Stimulated cells with PLD inhibitor were stained with annexin V to evaluate cell death (upper panel) and de-polarization of the mitochondria membrane was analyzed (lower panel). C: Thirty micrograms of cell extract was subjected to western blotting to measure the protein levels of microtubule-associated protein 1 light chain 3 alpha (LC3A) and microtubule-associated protein 1 light chain 3 beta (LC3B). Glyceraldehyde-3-phosphate dehydrogenase (GAPDH) was used as internal control. Data shown are the average of triplicate determinations±SD and are representative of three independent experiments. *$p<0.05$ vs. controls.*

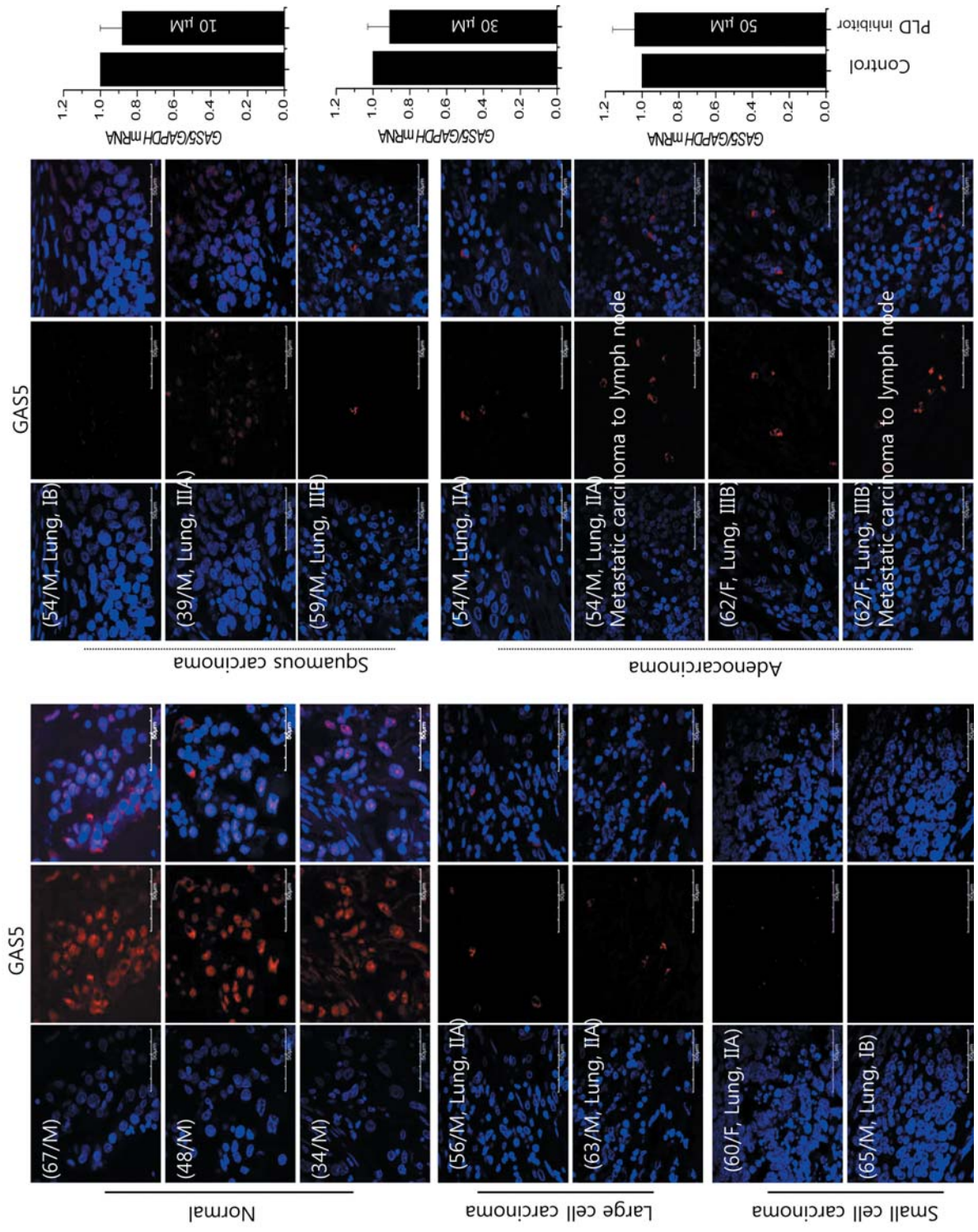

Figure 2. *Phospholipase D (PLD) inhibitor did not affect growth arrest-specific transcript (GAS5) expression. Lung cancer tissue array was subjected to in situ hybridization using antisense noncoding RNA in the INK4 locus (ANRIL) conjugated with red fluorescent protein (left panel) and H460 cells were treated with PLD inhibitor at the indicated concentrations for up to two days amd subjected to real-time polymerase chain reaction to evaluate the expression level of GAS5. Expression was plotted as the fold change that of the control. Data shown are the average of triplicate determinations ± SD and are representative of two or three independent experiments.*

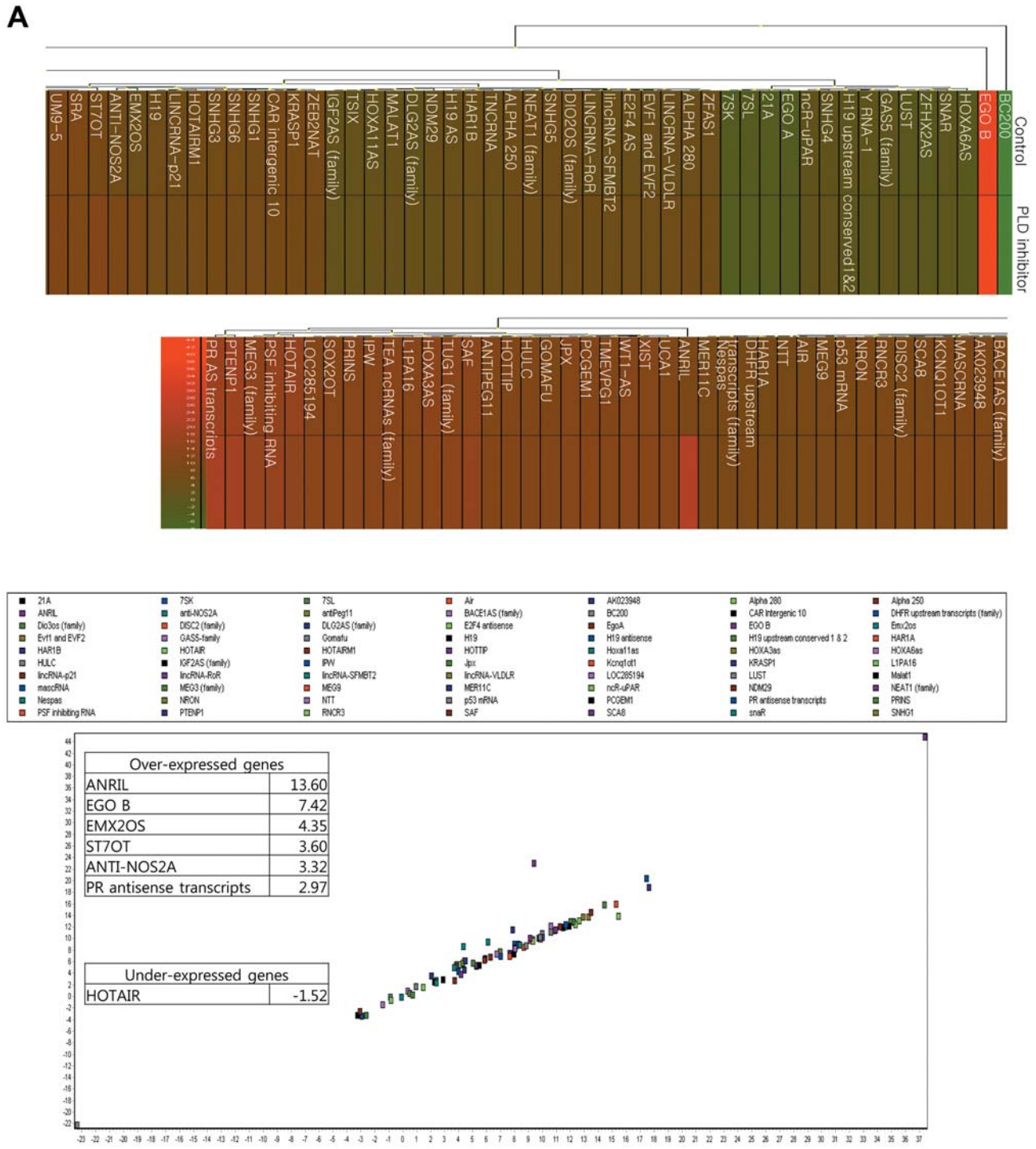

Figure 3. *Continued*

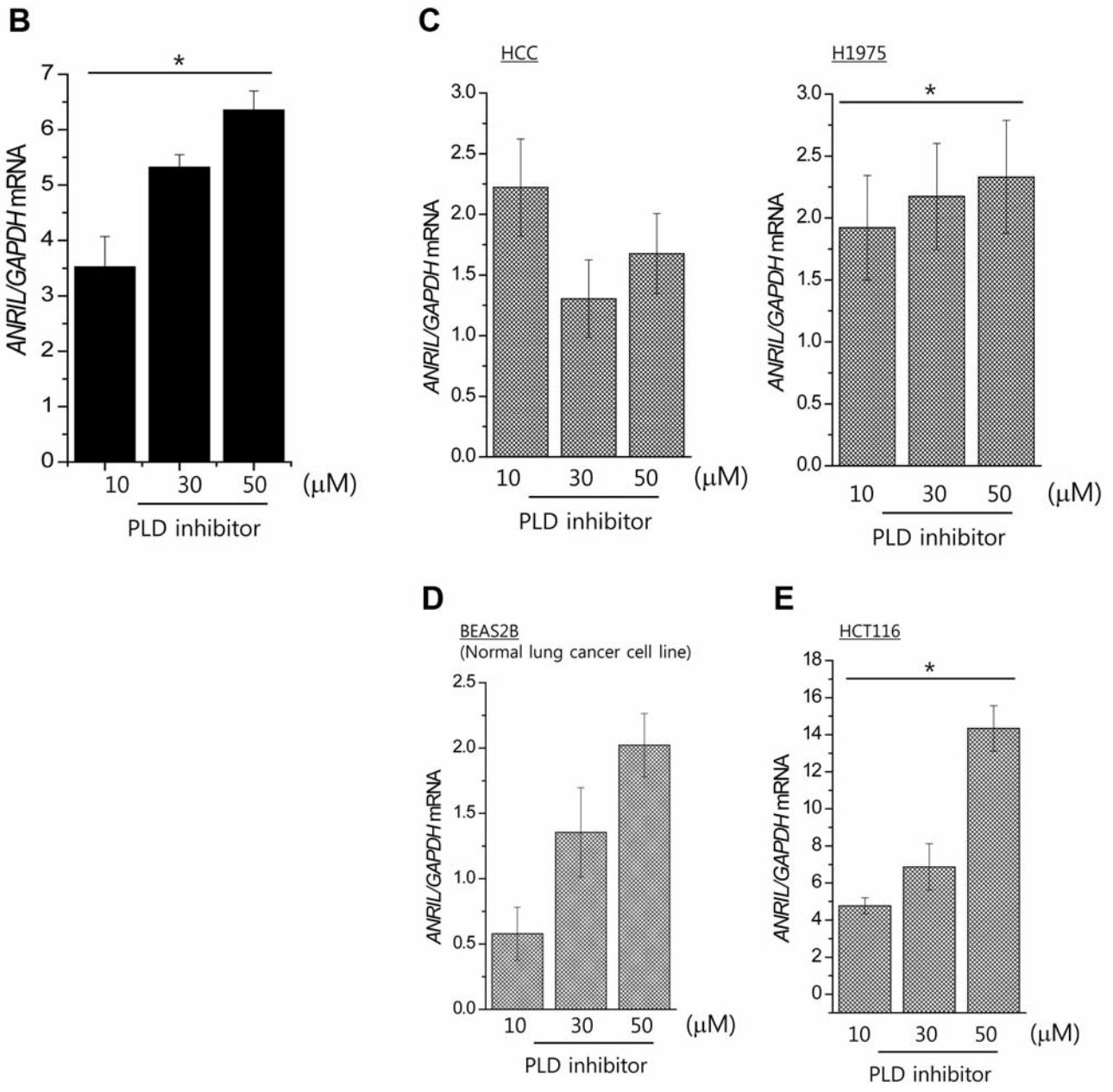

Figure 3. *Phospholipase D (PLD) inhibitor induces antisense non-coding RNA in the INK4 locus (ANRIL) expression. A: Long non-coding RNA (lncRNA) profiling was analyzed in H460 cells in the presence and absence of PLD inhibitor and expression values are represented as heatmap (upper panel) and plot (lower panel) using the software provided by manufacturers. H460 cells (B), HCC and H1975 cells (C), BEAS2B cells (D), or HCT116 cells were treated with PLD inhibitor at the indicated concentrations for up to two days and subjected to real-time polymerase chain reaction to evaluate the expression level of ANRIL. Expression was plotted as the fold change that of the control. Data shown are the average of triplicate determinations±SD and are representative of three independent experiments.*

provides evidence to support that dysregulation of lncRNA is linked to the anti-tumorigenesis *via* PLD inhibition.

In recent years, a large number of lncRNAs have been identified and there is an exponential growth of studies on the biological functions of lncRNAs in various types of human cancers (22). Even though fundamental and significant questions regarding lncRNAs in pathological mechanisms remain unanswered, investigation on lncRNAs is providing new opportunities to further our understanding over human diseases and to develop new treatments (23).

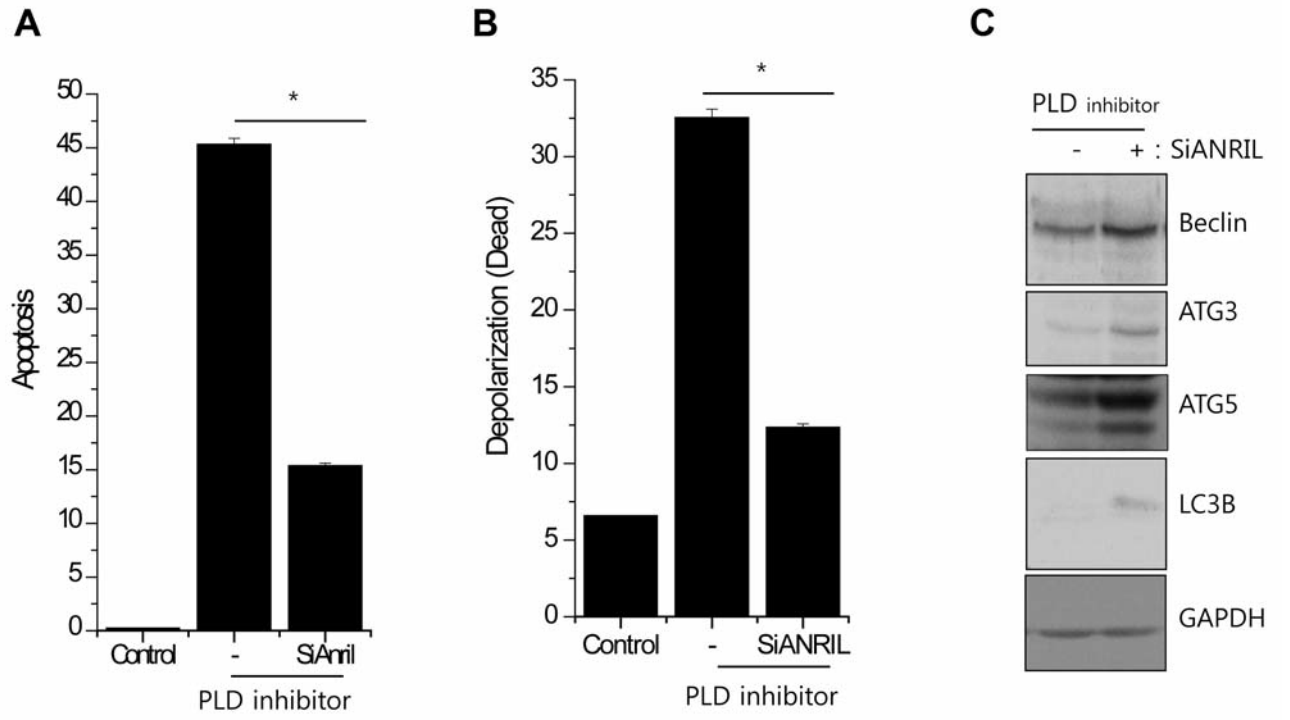

Figure 4. *Knockdown of antisense non-coding RNA in the INK4 locus (ANRIL) abrogated the anti-tumorigenic effects induced by Phospholipase D (PLD) inhibitor. H460 cells were transfected with ANRIL-specific siRNA in the presence and absence of PLD inhiibitor. A: Cells were analyzed for DNA content by propidium iodide staining and fluorescence-activated cell sorting (FACS) and the percentage of apoptosis is represented as a bar graph. B: Depolarization of the mitochondria membrane was analyzed. C: Cell extract (30 to 40 μg) was subjected to western blotting to measure the protein levels of coiled-coil myosin-like BCL2-Interacting Protein (BECLIN-1), autophagy-related gene 3 (ATG3), autophagy-related gene 5 (ATG5) and microtubule-Associated protein 1 light chain 3 Beta (LC3B). Glyceraldehyde-3-phosphate dehydrogenase (GAPDH) was used as internal control. Data shown are the average of triplicate determinations±SD and are representative of three independent experiments. *p<0.05 vs. controls.*

In the present study, significant up-regulation of *ANRIL* by PLD inhibition in cancer cells was shown. ANRIL is transcribed and spliced in a complex pattern (24, 25) and plays roles in a wide variety of cellular functions such as proliferation, apoptosis, migration, and extracellular matrix remodeling (26). Moreover, an increasing number of alternatively spliced *ANRIL* isoforms were reported for different cell types (27, 28), with unknown biological functions (29). A recent study showed overexpression of *ANRIL* altered expression of various genes involved in chromatin regulation (30), suggesting the functions of ANRIL may be diverse. Since the chromosomal region carrying *ANRIL* also carries cyclin-dependent kinase 2A and 2B, *ANRIL* is known to affect cell proliferation and apoptosis (31). ANRIL depletion triggered the up-regulation of the anti-apoptotic proteins, BCL2-related protein A1 (BCL2A1) and Baculoviral IAP repeat containing 3 (BIRC3) in vascular smooth muscle cells (32). However, the underlying regulatory mechanism of this non-coding RNA in lung cancer is poorly understood. Our results show that PLD inhibition induces antitumorigenesis by up-regulation of apoptosis and autophagy. Moreover, this effect involves lncRNA *ANRIL*. Our study furthers our understanding over the role of *ANRIL* and provides a potential therapeutic approach for controlling lung cancer.

Conflicts of interest

The Authors declare there exist no conflicts of interest.

Acknowledgements

This works was supported by National Research Foundation (NRF) of Korea Grant funded by the Korea government (MSIP) [2013R1A1A2011999, 2013R1A2A201067194, and 2011-0030130]. The funders had no role in study design, data collection and analysis, decision to publish, or preparation of the manuscript.

References

1 Liu Y, Li M, Zhang G and Pang Z: MicroRNA-10b overexpression promotes non-small cell lung cancer cell proliferation and invasion. Eur J Med Res *18(1)*: 41-48, 2013.

2 Willis BC, duBois, RM and Borok Z: Epithelial origin of myofibroblasts during fibrosis in the lung. Proc Am Thorac Soc *3(4)*: 377-382, 2006.

3 Su W, Chen Q and Frohman MA: Targeting phospholipase D with small-molecule inhibitors as a potential therapeutic approach for cancer metastasis. Future Oncol *5(9)*: 1477-1486, 2009.
4 Kang DW, Choi KY and Min do S: Phospholipase D meets Wnt signaling: a new target for cancer therapy. Cancer Res 71(2): 293-297, 2011.
5 Esteller M: Non-coding RNAs in human disease. Nat Rev Genet *12(12)*: 861-874, 2011.
6 Hatley ME, Patrick DM, Garcia MR, Richardson JA, Bassel-Duby R, van Rooij E and Olson EN: Modulation of K-Ras-dependent lung tumorigenesis by MicroRNA-21. Cancer Cell *18(3)*: 282-293, 2010.
7 Acunzo M1, Romano G, Palmieri D, Laganá A, Garofalo M, Balatti V, Drusco A, Chiariello M, Nana-Sinkam P and Croce CM: Cross-talk between MET and EGFR in non-small cell lung cancer involves miR-27a and Sprouty2. Proc Natl Acad Sci USA *110(21)*: 8573-8578, 2013.
8 Kutay H, Bai S, Datta J, Motiwala T, Pogribny I, Frankel W, Jacob ST and Ghoshal K: Down-regulation of miR-122 in the rodent and human hepatocellular carcinomas. J Cell Biochem *99(3)*: 671-678, 2006.
9 Anand S1, Majeti BK, Acevedo LM, Murphy EA, Mukthavaram R, Scheppke L, Huang M, Shields DJ, Lindquist JN, Lapinski PE, King PD, Weis SM and Cheresh DA: MicroRNA-132-mediated loss of p120RASGAP activates the endothelium to facilitate pathological angiogenesis. Nat Med *16(8)*: 909-914, 2010.
10 Fatica A and Bozzoni I: Long non-coding RNAs: new players in cell differentiation and development. Nat Rev Genet *15(1)*: 7-21, 2014.
11 Spizzo R, Almeida MI, Colombatti A and Calin GA: Long non-coding RNAs and cancer: A new frontier of translational research? Oncogene *31(43)*: 4577-4587, 2012.
12 Martens-Uzunova ES, Böttcher R, Croce CM, Jenster G, Visakorpi T and Calin GA: Long Noncoding RNA in Prostate, Bladder and Kidney Cancer. Eur Urol *65(6)*: 1140-1151, 2014.
13 Zhang Q, Su M, Lu G and Wang J: The complexity of bladder cancer: long noncoding RNAs are on the stage. Mol Cancer *12(1)*: 101-108, 2013.
14 Marks LS and Bostwick DG: Prostate cancer specificity of PCA3 gene testing: Examples from clinical practice. Rev Urol *10(3)*: 175-181, 2008.
15 Benetatos L, Vartholomatos G and Hatzimichael E: MEG3 imprinted gene contribution in tumorigenesis. Int J Cancer *129(4)*: 773-779, 2011.
16 Ying L, Chen Q, Wang Y, Zhou Z, Huang Y and Qiu F: Up-regulated *MALAT-1* contributes to bladder cancer cell migration by inducing epithelial-to-mesenchymal transition. Mol Biosyst *8(9)*: 2289-2294, 2012.
17 Ono H1, Motoi N, Nagano H, Miyauchi E, Ushijima M, Matsuura M, Okumura S, Nishio M, Hirose T, Inase N and Ishikawa Y: Long noncoding RNA HOTAIR is relevant to cellular proliferation, invasiveness and clinical relapse in small-cell lung cancer. Cancer Med *3(3)*: 632-642, 2014.
18 Rubio-Somoza I, Weigel D, Franco-Zorilla JM, Garcia JA and Paz-Ares J: ceRNAs: miRNA target mimic mimics. Cell *147(7)*: 1431-1432, 2011.
19 Sun Y and Chen J: mTOR signaling: PLD takes center stage. Cell Cycle *7(20)*: 3118-3123, 2008.
20 Shi X1, Sun M, Liu H, Yao Y, Kong R, Chen F and Song Y: A critical role for the long non-coding RNA GAS5 in proliferation and apoptosis in non-small-cell lung cancer. Mol Carcinog DOI 10.1002/mc.22120, 2013.
21 Park JB1, Lee CS, Jang JH, Ghim J, Kim YJ, You S, Hwang D, Suh PG and Ryu SH: Phospholipase signalling networks in cancer. Nat Rev Cancer *12(11)*: 782-792, 2012.
22 Xu MD, Qi P and Du X: Long non-coding RNAs in colorectal cancer: implications for pathogenesis and clinical application. Mod Pathol *27(10)*: 1310-1320, 2014.
23 Wapinski O and Chang HY: Long noncoding RNAs and human disease. Trends Cell Biol *21(6)*: 354-361, 2011.
24 Burd CE, Jeck WR, Liu Y, Sanoff HK, Wang Z and Sharpless NE: Expression of linear and novel circular forms of an INK4/ARF-associated non-coding RNA correlates with atherosclerosis risk. PLoS Genet *6(12)*: e1001233, 2010.
25 Folkersen L1, Kyriakou T, Goel A, Peden J, Mälarstig A, Paulsson-Berne G, Hamsten A, Hugh Watkins, Franco-Cereceda A, Gabrielsen A and Eriksson P: Relationship between CAD risk genotype in the chromosome 9p21 locus and gene expression. Identification of eight new *ANRIL* splice variants. PLoS One *4(11)*: e7677, 2009.
26 Congrains A, Kamide K, Ohishi M and Rakugi H: ANRIL: Molecular Mechanisms and Implications in Human Health. Int J Mol Sci *14(1)*: 1278-1292, 2013.
27 Pasmant E, Laurendeau I, Héron D, Vidaud M, Vidaud D and Bièche I: Characterization of a germ-line deletion, including the entire INK4/ARF locus, in a melanoma-neural system tumor family: identification of *ANRIL*, an antisense noncoding RNA whose expression coclusters with ARF. Cancer Res *67(8)*: 3963-3969, 2007.
28 Cunnington MS, Santibanez Koref M, Mayosi BM, Burn J and Keavney B: Chromosome 9p21 SNPs associated with multiple disease phenotypes correlate with ANRIL expression. PLoS Genet *6(4)*: e1000899, 2010.
29 Salzman J, Gawad C, Wang PL, Lacayo N and Brown PO: Circular RNAs are the predominant transcript isoform from hundreds of human genes in diverse cell types. PLoS One *7(2)*: e30733, 2012.
30 Sato K, Nakagawa H, Tajima A, Yoshida K and Inoue I: ANRIL is implicated in the regulation of nucleus and potential transcriptional target of E2F1. Oncol Rep *24(3)*: 701-707, 2010.
31 Matheu A, Maraver A, Collado M, Garcia-Cao I, Cañamero M, Borras C, Flores JM, Klatt P, Viña J and Serrano M: Anti-aging activity of the *Ink4/Arf* locus. Aging Cell *8(2)*: 152-161, 2009.
32 Congrains A, Kamide K, Katsuya T, Yasuda O, Oguro R, Yamamoto K, Ohishi M and Rakugi H: CVD-associated non-coding RNA, *ANRIL*, modulates expression of atherogenic pathways in VSMC. Biochem Biophys Res Commun *419(4)*: 612-616, 2012.

Received February 2, 2015
Revised February 17, 2015
Accepted February 20, 2015